EARTH SURFACE PROCESSES AND LANDFORMS
Earth Surf. Process. Landforms **38**, 179–182 (2013)

Published online 20 September 2012 in Wiley Online Library
(wileyonlinelibrary.com) DOI: 10.1002/esp.3316

Analysis of transverse aeolian ridge profiles derived from HiRISE images of Mars

K. M. Shockey and J. R. Zimbelman*
Center for Earth Planetary Studies National Air Space Museum, MRC 315, Smithsonian Institution, Washington, DC, USA

Received 2 May 2011; Revised 6 July 2012; Accepted 8 August 2012

*Correspondence to: James Zimbelman, Center for Earth and Planetary Studies, National Air and Space Museum, MRC 315, Smithsonian Institution, Washington, DC, 20013–7012, USA. E-mail: zimbelmanj@si.edu

ESPL
Earth Surface Processes and Landforms

ABSTRACT: Photoclinometry was used to analyze selected High Resolution Imaging Science Experiment (HiRISE) images of Transverse Aeolian Ridges (TARs) on Mars. Sixty Mars profiles have been assessed and a summary of their morphologic characteristics compiled. Measurements collected quantified the symmetry of the feature, the curvature of the crest, flank slopes, width, height and several comparative ratios. Results show that small TARs have physical characteristics generally similar to measurements obtained from lower resolution images of Mars. The HiRISE image data allow for much improved sampling along each feature; the improved resolution reveals relatively few features not seen in earlier studies, but is well suited for topographic sampling. Measured TAR profiles, when scaled by the width of the feature, can be compared to similarly scaled profiles for terrestrial dunes and megaripples. Published 2012. This article is a U.S. Government work and is in the public domain in the USA.

KEYWORDS: reversing dunes; megaripples; photoclinometry; TARs; geomorphology

Introduction

High Resolution Imaging Science Experiment (HIRISE) images have revealed surface features on Mars that had not been seen previously at the meter scale, through the highest resolution yet obtained from orbit (McEwen *et al.*, 2007). Topographic data other than what can be derived from HiRISE stereo pairs (Kirk *et al.*, 2008; Lewis *et al.*, 2008) have yet to reach a resolution comparable with that of individual HiRISE images, except at sites investigated by landers or rovers (Squyres *et al.*, 2004a, 2004b). Photoclinometry (shape from shading) is a tool that can derive topographic profile information along selected lines within HiRISE images. HiRISE images already have significantly influenced the study of Transverse Aeolian Ridges (TARs) (Shockey and Zimbelman, 2010; Zimbelman, 2010; Berman *et al.*, 2011), which have been previously interpreted to be produced either as small dunes or large ripples (Wilson and Zimbelman, 2004; Balme *et al.*, 2008; Shockey *et al.*, 2008; Zimbelman, 2010; Berman *et al.*, 2011).

Background

TARs typically have high to medium albedo (relative to their surroundings), generally linear to arcuate crests, and are observed globally on Mars but they are more common in equatorial and southern mid-latitudes than in polar regions, based on studies of thousands of Mars Orbiter Camera (MOC) images (Wilson and Zimbelman, 2004; Balme *et al.*, 2008). At least some TARs appear to be more abundant near the dichotomy boundary (Shockey *et al.*, 2008) and in proximity to layered terrains (Balme *et al.*, 2008; Berman *et al.*, 2011). In the present study, simplified photoclinometry was used to derive topographic profiles from several HiRISE images that included many examples of TARs. Photoclinometry involves the inference of surface relief from the brightness of individual picture elements (pixels) in digital image data, and it has been applied successfully to a wide variety of spacecraft images under varying assumptions of the photometric properties of the surface (Wildey, 1975; Jankowski and Squyres, 1991; Kirk *et al.*, 2008). Here two important assumptions were made before applying simplified photoclinometry to the areas of investigation (Zimbelman, 2010); (1) the albedo of the surface remains constant along the entire line, and (2) the photometric properties of the surface materials are taken to be Lambertian, where reflected brightness is solely dependent upon the solar incidence angle to the surface and not dependent on emission angle. Profiles were kept relatively short (<10s of meters) in order to minimize potential errors resulting from albedo variations over longer distances Jankowski and Squyres (1991). Profile locations were purposely chosen to minimize potential albedo effects; that is, we selected TARs for measurement that did not show discernable albedo variations along the entire line. Several classification systems have been used to describe TARs (Wilson and Zimbelman, 2004; Balme *et al.*, 2008; Shockey *et al.*, 2008; Shockey and Zimbelman, 2010); the classification system described by Balme *et al.* (2008) was followed here while considering the TARs examined in this study.

Methods

Five widely dispersed HiRISE images (PSP_009754_1450, PSP_009718_2005, PSP_009604_1725, PSP_007640_1300, ESP_019261_1410; Figure 1) in jp2 format were used to obtain measured profiles, in order to characterize the topography across individual TARs. The selected images come from evaluation of hundreds of HiRISE frames; the ones chosen for study had well-expressed abundant fields of TARs, and we made an effort to select study locations not closely associated with major topographic obstacles. From these images, 60 individual profiles were collected perpendicular to the crest orientation in order to determine the width, height, and overall symmetry of each TAR, as well as obtaining the first evaluation of the 'sharpness' of TAR crests (measured and derived attributes are listed for each individual TAR profile in the Supplementary Information data file accompanying this manuscript). Images used in this study have either 25 or 50 cm/pixel spatial resolution (see Supplementary Information data file for details about each image), so that differences between two points along an individual profile are likely reproducible to about 1 m for all profile measurements presented here.

Calibrated reflected brightness values were collected for each pixel along a line perpendicular to the TAR crest using ImageJ (public domain software available from http://rsbweb.nih.gov/ij/), which was then imported into Excel to carry out the photoclinometric determination of surface slope derived from the image reflectance relative to that of a uniform (flat) horizontal surface (Zimbelman, 2010). Figure 2 shows an example of three line locations on a subsection from one HiRISE image (with contrast increased for clarity), from which individual topographic profiles were derived. Note that no true shadows are present along the profile locations, so that slopes can be confidently inferred from the surface brightness. Typically a single TAR was selected from each profile for analysis, based on which feature best represented the TARs sampled along the line (Figure 3). All surveyed lines were measured consistently from north and/or west to the south and/or east. Width was measured from the basal break in slope on both sides of the crest of each TAR, inferred from the topographic profile (following Zimbelman, 2010); e.g. width was measured from point A to point E in Figure 4. Height was measured from the crest to the midpoint between the troughs on either side of the crest (in Figure 4, point C to halfway between A and E); this procedure for determining height eliminates the need to remove the effect of regional slope from the profile. The height-to-width ratio is the single quantity that has proved to be the most useful for characterizing the overall aspect ratio of a variety of aeolian features (Zimbelman *et al.*, 2010; Zimbelman *et al.*, 2012). The average slope for each TAR was determined by taking the arc-tangent of twice the height divided by the width.

The symmetry of the TAR was quantified here by determining the midpoint between the two points used to represent the width of the feature, and then determining if the crest was directly over this mid-point. If the crest was located directly over the midpoint, then the symmetry was given a value of zero and the TAR was perfectly symmetric. If the crest was not over the midpoint, then the horizontal distance between the crest and the midpoint was determined; this result could be either negative (left-leaning) or positive (right-leaning), though this leaning direction remains somewhat subjective. To remove this subjectivity, the absolute value of the symmetry distance was used, divided by the feature width to give a size-independent scaled ratio of the asymmetry; the larger the scaled ratio, the greater the asymmetry of the TAR. Note that this symmetry assessment does not consider minor breaks in slope on the sides of the feature, but perhaps recent wind direction might contribute to regional consistency in TAR asymmetries. Also note that parallax may affect the derived symmetry value in off-nadir images (see Discussion section below).

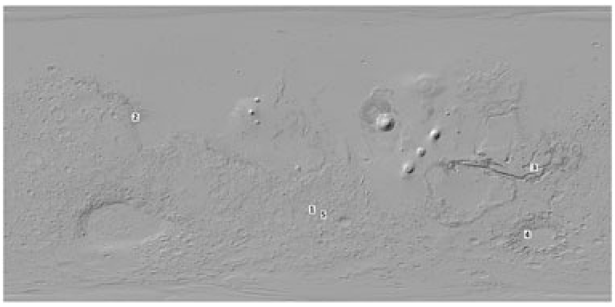

Figure 1. Location of the five HiRISE images used in this study, shown on a shaded relief version of MOLA topography. Numbers indicate the following HiRISE frames: 1 – PSP_009754_1450, 50 cm/p; 2 – PSP_009718_2005, 25 cm/p; 3 – PSP_009604_1725, 25 cm/p; 4 – PSP_007640_1300, 50 cm/p; 5 – ESP_019261_1410, 50 cm/p.

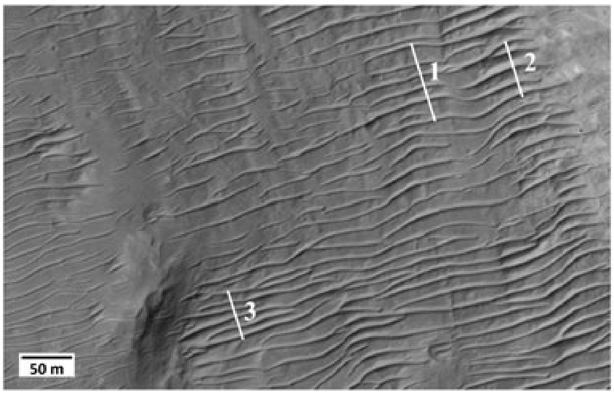

Figure 2. Subscene of HIRISE image PSP_009604_1725 showing the locations of three profiles across TARs. North is to the top. See Figure 3 for the profile along line 1. NASA/JPL/U of A.

The possible recent dynamic state of a TAR can be considered by studying how sharp the crest is. To quantify the sharpness of the crest, three points were used. The central point is at the crest (point C in Figure 4), with two additional points from either side of the crest (B and D in Figure 4); the side points were selected by inspection, where crest curvature appeared to terminate at relatively straight flanks, also chosen to be equidistant from the crest point. These three points were then used to calculate the size of an inscribed circle (within the plane of the profile) that included all three points, whose radius was then divided by the width of the TAR to produce a size-independent indication of crest sharpness. The 'crest ratio' can be interpreted such that the smaller the number, the sharper the crest of the TAR.

Results

From the 60 Mars profiles that have been assessed here (see Supplementary Information for details derived from each profile), several morphologic characteristics of TARs were constrained. The average width for all of the measured TARs is 22.6 m, with a maximum of 107 m and a minimum of 4.5 m, but the majority of widths fall in the range 15 to 30 m. Wilson and Zimbelman (2004) measured TAR wavelength rather than feature width, but Balme *et al.* (2008) documented 'downwind length' of TARs that is quite comparable with the widths obtained here. The average height of the profiled TARs was determined to be 2.3 m, with a maximum of 9.7 m and a minimum of 0.3 m, but the greatest concentration of heights were in the range 0.5 to 5 m. Height is definitely the most difficult feature attribute to measure accurately on Mars (Bourke *et al.*, 2006). The height results obtained here are quite consistent with previous estimates of <1.5 m (Zimbelman, 2000), ~5.7 m

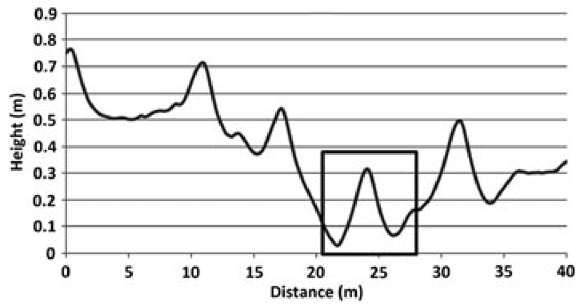

Figure 3. Profile obtained along line 1 in Figure 2. Box corresponds to the individual TAR shown in Figure 4.

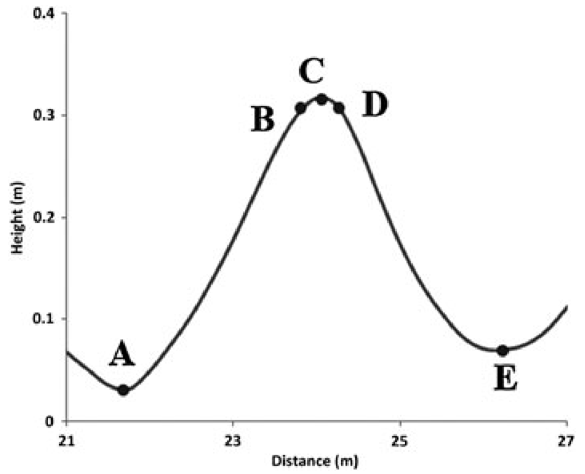

Figure 4. Example of measurements made from a TAR profile (see box in Figure 3). Points A through E are used in deriving several measured attributes of the feature (see text).

(for TARs of wavelength ~38 m; Williams *et al.*, 2003), and 1 to 7.8 m (Bourke *et al.*, 2006), all obtained using a variety of techniques. Importantly, the measured TAR heights fall within the range of heights measured on a wide range of terrestrial megaripples and transverse (reversing) sand dunes (Zimbelman and Williams, 2007; Zimbelman *et al.*, 2012). Measured HiRISE profiles with both vertical height and horizontal distance scaled by feature width prove useful for distinguishing between probable reversing dune and megaripple origins for TARs (Zimbelman, 2010); the results obtained here support the previously published interpretation (based on a limited sample size) that TARs with heights <0.5 m are more likely megaripples while TARs with heights >1 m are more likely reversing sand dunes.

The height/width ratio for the TARs measured here averaged 0.12, with a maximum of 0.29 and a minimum of 0.008. These height/width values are quite consistent with values measured on terrestrial reversing dunes (Zimbelman *et al.*, 2012), although the actual width of the Martian TARs tends to be smaller than the width of most terrestrial reversing dunes. The slopes on both sides of the TARs were nearly equal to the overall average slope (another indication of the symmetry of the features); slopes yielded an average value of 14.5°, with a maximum of 38.1° (a value slightly higher than the angle of repose, suggesting either that the value is an overestimate or that some form of induration may allow some slopes to steepen slightly beyond the angle of repose) and with a minimum at 0.9°, a value suggesting that a small number of TARs may consist of a rather limited quantity of particles.

The symmetry results are the first such measurements reported for TARs. Symmetry ratios yielded an average of 0.09, indicating that TARs are indeed very symmetric features, with a maximum of 0.3 and a minimum of 0 (perfectly symmetric). More than 10% of the symmetry ratios were perfectly symmetric, and the vast majority of all profiles were very nearly symmetrical; these results, derived from TARs widely distributed around Mars, supports the interpretation that symmetric profiles are an important attribute of TARs, one that is most consistent with a reversing dune origin (Zimbelman, 2010). Sharpness of the TAR crest, represented by the crest ratio, had a value <1 for one-third of the profiles, the majority of the values are <4, with a maximum value of 981 (indicating a relatively flat top; only four profiles had ratios >100, all from frame 7640, obtained at a high southern mid-latitude) and a minimum value of 0.09. In aggregate, the TAR crest ratios indicate that many crests are not particularly 'sharp' features, which is indirect support for previous results which indicate that TARs are not active under current conditions (Balme *et al.*, 2008; Berman *et al.*, 2011).

Discussion

The results presented here provide a basis for expanding upon previous MOC-based studies of TARs (Wilson and Zimbelman, 2004; Balme *et al.*, 2008; Berman *et al.*, 2011). Unlike these previous studies, the present work focuses on the profile characteristics of individual TARs rather than on attributes of fields or large groups of TARs. Whereas earlier studies used properties derived from a plan view of TAR crests (e.g. total crest length, types of crest branching, angles of crest interaction, etc.), our work has focused on measurable attributes along a line perpendicular to the TAR crest. These new results are thus quite literally 'orthogonal' to most previously published descriptions of TARs. Compared with the observations of Wilson and Zimbelman (2004), the present study investigated TARs with a typical wavelength that is about one-half of what was possible from using MOC images. Previous investigations of the scaling of TAR measurements revealed that wavelength was often too variable, even within a single TAR field, to provide a consistent parameter to compare features at different locations (Zimbelman and Williams, 2008), which led to the use of feature width as the basis for scaling profiles for comparison (Zimbelman, 2010).

Beyond the demonstrated documentation of TARs smaller than those confidently identified in MOC images, the HiRISE data now provide many more measured points across an individual TAR than was previously possible, which in turn allows for investigation of attributes such as feature symmetry. Unfortunately, measurements of characteristics such as symmetry and crest sharpness are not (yet) available in the literature, either for Mars or for terrestrial aeolian features, although our work demonstrates that such comparisons are now possible. A companion paper provides profile measurements of terrestrial sand ripples, megaripples, and reversing sand dunes (Zimbelman *et al.*, 2012) that provides a basis for future comparison of TAR profile attributes to an array of terrestrial aeolian features. Investigations making use of early HiRISE results (Bridges *et al.*, 2007; Zimbelman, 2010; Berman *et al.*, 2011) revealed many of the general characteristics of TARs (a preference for being located within broad topographic lows, little surface textural information other than smaller-order ripples superposed on the sides of TARs, interactions with surrounding topography, etc.), but without the means to quantify various aspects of TAR topography. Study of the shape of individual TARs (including quantifying their shape characteristics) through the use of HiRISE images (first illustrated in Zimbelman, 2010) provides a powerful tool for investigating the wide-spread but still enigmatic TAR features. HiRISE images also provide the opportunity to expand upon the TAR classification system derived by Balme *et al.* (2008), but such an effort is well beyond the scope of the project that provided support for the work presented here.

The potential effect of parallax in off-nadir images must be considered when evaluating image-based results. The vertical relief of a feature can produce altered horizontal dimensions when measured from non-ortho-rectified images; such a rectified product is difficult to obtain for most users of HiRISE images, as well as for imaging data from many orbital platforms. Four of the five HiRISE images used here are within 1° of nadir (see Supplementary data file), where potential parallax issues should be <1% (order of magnitude). However, four measured profiles from the remaining image could have parallax issues at the 3% to 5% level (these four profiles are flagged in the supplementary data file). Readers are urged to pay particular attention to the emission angle of images under consideration for analyses such as those presented here; photoclinometry results will be most robust for images obtained as close to nadir as possible.

Future Work

Future work should include analysis of more HiRISE images, to provide more comprehensive coverage of TARs from across the entire Martian surface, including measuring TARs larger than the features examined here. An assessment of whether or not these features are considered to have been recently active (e.g. impact craters superposed on TARs suggest that the features may not have been active recently; Berman *et al.*, 2011), as well as how degraded they are, may provide new insight into recent wind conditions in the study areas. Future efforts should examine the parallax issue for HiRISE images in detail, such as a comparison of results from both original and ortho-rectified images (where available). Profiles of larger features known to be dunes on Mars should be compared with TAR morphologic characteristics, including how the Martian dunes compare with both the terrestrial and Martian morphologic data already available. Comparison of results with the conclusions derived from previous studies will allow for an improved assessment of these features beyond what can be obtained from studies of Martian images in plan form only.

Acknowledgements—The comments of Simone Silvestro, an anonymous reviewer, and the Special Issue Editor Mark Bishop were very helpful during revision of the manuscript. This work was supported by NASA Mars Data Analysis Program grant NNX08AK90G (JRZ, PI).

Supporting Information

Supporting information may be found in the online version of this article.

References

Balme M, Berman DC, Bourke MC, Zimbelman JR. 2008. Transverse aeolian ridges (TARs) on Mars. *Geomorphology* **101**: 703–720. DOI: 10.106/j.geomorph.2008.03.011.

Berman DC, Balme MR, Rafkin SCR, Zimbelman JR. 2011. Transverse aeolian ridges (TARs) on Mars II: distributions, orientations, and ages. *Icarus* **213**: 116–130. DOI: 10.1016/j.icarus.2011.02.014.

Bourke MC, Balme MR, Beyer RA, Williams KK, Zimbelman JR. 2006. A comparison of methods used to estimate the height of sand dunes on Mars. *Geomorphology* **81**(3–4): 440–452.

Bridges NT, Geissler PE, McEwen AS, Thomson BJ, Chuang FC, Herkenhoff KE, Keszthelyi LP, Martínez-Alonso S. 2007. Windy Mars: A dynamic planet as seen by the HiRISE camera. *Geophysical Research Letters* **34**: L23205. DOI: 10.1029/2007GL031445.

Jankowski DG, Squyres SW. 1991. Sources of error in planetary photoclinometry. *Journal of Geophysical Research* **96**(E4): 20907–20922.

Kirk RL, *et al*. 2008. Ultrahigh resolution topographic mapping of Mars with MRO HiRISE stereo images: meter-scale slopes of candidate Phoenix landing sites. *Journal of Geophysical Research* **113**: E00A24. DOI: 10.1029/2007JE003000.

Lewis KW, Aharonson O, Grotzinger JP, Kirk RL, McEwen AS, Suer T. 2008. Quasi-periodic bedding in the sedimentary rock record of Mars. *Science* **322**: 1532–1535. DOI: 10.1126/science.1161870.

McEwen AS, Eliason EM, Bergstrom JW, Bridges NT, Hansen CJ, Delamere WA, Grant JA, Gulick VC, Herkenhoff KE, Keszthelyi L, Kirk LR, Mellon MT, Squyres SW, Thomas N, Weitz CM. 2007. Mars reconnaissance orbiter's High Resolution Imaging Science Experiment (HiRISE). *Journal of Geophysical Research* **112**: E05S02. DOI: 10.1029/2005JE002605.

Shockey KM, Zimbelman JR. 2010. Transverse Aeolian Ridges as seen in HiRISE Images. Lunar and Planetary and Science Conference XLI, Abstract #1423. Lunar and Planetary Institute: Houston.

Shockey KM, Zimbelman JR, Gregg TKP. 2008. Transverse Aeolian ridges across the dichotomy boundary of Mars. Lunar and Planetary and Science Conference XXXIX, Abstract #1686. Lunar and Planetary Institute: Houston.

Squyres SW, *et al*. 2004a. The Spirit Rover's Athena science investigations at Gusev crater, Mars. *Science* **305**: 794–799.

Squyres SW, *et al*. 2004b. The Opportunity Rover's Athena science investigation at Meridiani Planum, Mars. *Science* **306**: 1698–1703.

Wildey RL. 1975. Generalized photoclinometry for Mariner 9. *Icarus* **25**(4): 613–626.

Williams KK, Greeley R, Zimbelman JR. 2003. Using overlapping MOC images to search for dune movement and to measure dune heights. Lunar and Planetary Science Conference XXXIV, Abstract #1639. Lunar and Planetary Institute: Houston.

Wilson SA, Zimbelman JR. 2004. The latitude-dependent nature and physical characteristics of transverse aeolian ridges on Mars. *Journal of Geophysical Research* **109**: E10003. DOI: 10.1029/2004JE002247.

Zimbelman JR. 2000. Non-active dunes in the Acheron Fossae region of Mars between the Viking and Mars Global Surveyor eras. *Geophysical Research Letters* **27**(7): 1069–1072.

Zimbelman JR. 2010. Transverse aeolian ridges on Mars: first results from HiRISE images. *Geomorphology* **121**: 22–29. DOI: 10.1016/j.geomorph.2009.05.012.

Zimbelman JR, Williams SH. 2007. Dunes versus ripples: topographic profiling across terrestrial examples, with application to the interpretation of features on Mars. *EOS Transactions of the American Geophysical Union* **88**(23), Joint Assembly Supplement, Abstract P34A–07.

Zimbelman JR, Williams SH. 2008. Inferences about sand dunes on Mars derived from the analysis of two HiRISE images. Lunar and Planetary and Science Conference XXXIX, Abstract #1699. Lunar and Planetary Institute: Houston.

Zimbelman JR, Williams SH, Johnston AK. 2010. Cross-sectional profiles of ripples, megaripples, and dunes: a method for discriminating between formational mechanisms. Second International Planetary Dunes Workshop, LPI Contribution No. 1552: 76–77. Lunar and Planetary Institute: Houston.

Zimbelman JR, Williams SH, Johnston AK. 2012. Cross-sectional profiles of sand ripples, megaripples, and dunes: a method for discriminating between formational mechanisms. *Earth Surface Processes and Landforms* **37**: 1120–1125. DOI: 10.1002/esp.3243.

